The local variational multiscale method

S. Scott Collis[a,*], Srinivas Ramakrishnan[b]

[a] Optimization and Uncertainty Estimation, Sandia National Laboratory†, Albuquerque, NM 87185–0370, USA
[b] Mechanical Engineering and Materials Science, Rice University, Houston, TX 74005, USA

Abstract

Combining the variational multiscale (VMS) method for large-eddy simulation with a discontinuous Galerkin (DG) spatial discretization leads to a synergistic approach to turbulence simulation that we call the local variational multiscale (ℓVMS) method. In ℓVMS the flexibility of DG enables the large and small-scale spaces to be set on each element independently. In this paper, preliminary results using ℓVMS are presented for turbulent channel flow that demonstrate the flexibility and efficacy of the method.

Keywords: Multiscale; Large eddy simulation; Turbulence; Variational multiscale

1. Introduction

Continuing our study of discontinuous Galerkin (DG) methods for simulating turbulent flows, the current paper builds upon several recent publications that document our progress to date [1,2,3,4]. The focus of this paper is to present preliminary results for the combination of DG and the variational multiscale (VMS) method for large eddy simulation (LES) [5,6,7] – a synergistic combination we call the local variational multiscale (ℓVMS) method that is promising for LES in complex geometries.

We begin with a brief discussion of the formulation and implementation of ℓVMS for turbulence simulation. Although ℓVMS is particularly attractive for flows in complex geometries [1,2], as a first step, this paper presents ℓVMS results for planar turbulent channel flow to demonstrate the validity of the approach. The paper concludes with a summary of our findings and a discussion of future research directions.

* Corresponding author. Tel.: +1 (505) 2841123; Fax: +1 (505) 2840154; E-mail sscoll@sandia.gov

† Sandia is a multiprogram laboratory operated by Sandia Corporation, a Lockheed Martin Company, for the United States Department of Energy under contract DE-AC04-94AL85000

Computational Fluid and Solid Mechanics 2005
K.J. Bathe (Editor)

2. Formulation

Consider the compressible Navier–Stokes equations in strong form

$$\boldsymbol{U}_{,t} + \boldsymbol{F}_{i,i} - \boldsymbol{F}^{v}_{i,i} = \mathbf{S} \quad \text{in } \Omega \times (0,T) \tag{1a}$$

$$\boldsymbol{U}(x,0) = \boldsymbol{U}_0(\boldsymbol{x}) \quad \text{in } \Omega \tag{1b}$$

where $\boldsymbol{U} = \{\rho,\ \rho\boldsymbol{u},\ \rho e\}^T$ is the vector of conserved variables, ρ is the fluid density, $\boldsymbol{u}$ is the fluid velocity vector, and e is the total energy per unit mass. The inviscid and viscous flux vectors in the ith coordinate direction are $\boldsymbol{F}_i(\boldsymbol{U})$ and $\boldsymbol{F}^v_i(\boldsymbol{U})$, and S is a source term. Equation (1a) is solved subject to appropriate boundary conditions that must be specified for each problem of interest; a state equation, such as the ideal gas equation; and constitutive laws that define fluid properties such as viscosity and thermal conductivity as functions of the conserved variables. Due to space limitations, we do not explicitly define the flux vectors, state equation, or constitutive relations, but instead refer the reader to standard texts (see, e.g., [8]).

The fixed spatial domain for the problem is denoted by Ω, which is an open, connected, bounded subset of $\mathbb{R}^3$, with boundary $\partial\Omega$. Let $\mathcal{P}_h$ be a partition of the domain Ω into N subdomains Ω_e where

$$\bar{\Omega} = \bigcup_{e=1}^{N} \bar{\Omega}_e \quad \text{and} \quad \Omega_e \cap \Omega_f = \emptyset \quad \text{for} \quad e \neq f \tag{2}$$

Starting from the strong form of the compressible

Navier–Stokes equations (1a), we consider a single subdomain, Ω_e, multiply by a weighting function $\mathbf{W}$ that is continuous in Ω_e, and integrate the flux terms by parts

$$\int_{\Omega_e} \left(\boldsymbol{W}^T \boldsymbol{U}_{,t} + \boldsymbol{W}^T_{,i} (\boldsymbol{F}^v_i - \boldsymbol{F}_i) \right) d\boldsymbol{x} + \int_{\partial\Omega_e} \boldsymbol{W}^T (\boldsymbol{F}_n - \boldsymbol{F}^v_n)\, d\boldsymbol{s} = \int_{\Omega_e} \boldsymbol{W}^T \mathbf{S} d\boldsymbol{s} \tag{3}$$

where $\boldsymbol{F}_n = \boldsymbol{F}_i n_i$. In discontinuous Galerkin, one allows the solution and weighting functions to be discontinuous across element interfaces and the solutions on each element are coupled using appropriate numerical fluxes for both inviscid $\boldsymbol{F}_n(\boldsymbol{U}) \to \hat{\boldsymbol{F}}_n(\boldsymbol{U}^-, \boldsymbol{U}^+)$ and viscous fluxes, $\boldsymbol{F}^v_i(\boldsymbol{U}, \boldsymbol{U}_{,j}) \to \hat{\boldsymbol{F}}^v_i(\boldsymbol{U}^-, \boldsymbol{U}^-_{,j}, \boldsymbol{U}^+, \boldsymbol{U}^+_{,j})$. Introducing numerical fluxes and summing over all elements yields

$$\sum_{e=1}^{N} \int_{\Omega_e} \left(\boldsymbol{W}^T \boldsymbol{U}_{,t} + \boldsymbol{W}^T_{,i} (\boldsymbol{F}^v_i - \boldsymbol{F}_i) \right) d\boldsymbol{x} + \sum_{e=1}^{N} \int_{\partial\Omega_e} \boldsymbol{W}^T \left(\hat{\boldsymbol{F}}_n(\boldsymbol{U}^-, \boldsymbol{U}^+) \right) d\boldsymbol{s} - \sum_{e=1}^{N} \int_{\partial\Omega_e} \boldsymbol{W}^T \left(\hat{\boldsymbol{F}}^v_n(\boldsymbol{U}^-, \boldsymbol{U}^-_{,j}, \boldsymbol{U}^+, \boldsymbol{U}^+_{,j}) \right) d\boldsymbol{s} = \sum_{e=1}^{N} \int_{\Omega_e} \boldsymbol{W}^T \mathbf{S}\, d\boldsymbol{s} \tag{4}$$

where $\boldsymbol{U}^+$ and $\boldsymbol{U}^-$ are the adjacent and local states, respectively. For an element edge on the physical boundary $\partial\Omega$, $\boldsymbol{U}^+ = \boldsymbol{U}_{bc}$. Likewise, for inter-element boundaries, $\boldsymbol{U}^+$ comes from the neighboring element. Thus, all interface and boundary conditions are set through the numerical fluxes. We use the Lax–Friedrichs flux for the inviscid numerical flux and the method of Bassi et al. [9] for the viscous numerical flux. For a more thorough discussion of our approach, including boundary conditions, the interested reader is referred to [4].

For LES, we utilize the variational multiscale (VMS) method introduced by Hughes et al. [6] and recast in a form more consistent with traditional turbulence modeling by Collis [5]. This method bypasses several of the limitations of filter-based LES – such as filter-derivative commutation and filter design on inhomogeneous grids – by using variational projection to effect scale separation, thereby making extension to complex geometries easier.

The VMS methodology, involves a priori partitioning of the solution $\boldsymbol{U} = \bar{\boldsymbol{U}} + \tilde{\boldsymbol{U}} + \hat{\boldsymbol{U}}$ where $\bar{\boldsymbol{U}}$ are the large scales, $\tilde{\boldsymbol{U}}$ are the small scales, and $\hat{\boldsymbol{U}}$ are the unresolved scales [5]. Subsequently, equations for each scale range can be derived and the influence of the unresolved scales (through Reynolds and cross stresses) on the resolved scales can be isolated (see Collis [5] for details). Thereafter, a subgrid scale model confined to act just on the small scales, such as a constant coefficient Smagorinsky model, is introduced to model the influence of the unresolved scales on the resolved scales. This approach to modeling, where *no* explicit model is applied on the large scales, is responsible for the success of VMS, when using a constant coefficient Smagorinsky model on the small scales, in both equilibrium and non-equilibrium flows [7,10,11].

The discontinuous Galerkin method permits the use of unstructured grids with high-order, hierarchical representations used on each element that provides a convenient setting for VMS turbulence modeling. This makes the combination of DG and VMS (i.e. ℓVMS) particularly attractive for turbulence simulations in complex geometries and the reader is referred to [1,4,12] for more details regarding ℓVMS.

3. Numerical results

Consider fully-developed turbulent flow in a planar channel with streamwise x, wall-normal y, and spanwise z directions. The flow is assumed to be periodic in x and z where the box size is selected so that the turbulence is adequately decorrelated.

In Ramakrishnan et al. [4], DNS using DG discretizations highlighted the capabilities of DG in terms of local *hp*-refinement and weak boundary-conditions for efficiently simulating near-wall turbulence. The current paper, extends this work to include VMS consisting of a Smagorinsky model [6] applied only to small scales. As an initial demonstration of ℓVMS, simulations are presented at $Re_\tau = 100$ and 395 using a centerline Mach number of $M_c = 0.3$ so that comparisons can be made to prior incompressible results (see e.g. [13,14]). Following Coleman et al. [15], we use a cold, isothermal wall so that internal energy created by molecular dissipation is removed from the domain via heat transfer across the walls, allowing a statistically steady state to be achieved. The bulk mass flow is held constant by the addition of an x-momentum source on the right-hand side of Eq. (1a).

The computational parameters for each simulation are shown in Table 1 where L_i and N_i denote the domain size and the number of elements in the ith direction, respectively. The parameter p is the local polynomial order on each element which, for simplicity is taken to be uniform for the simulations presented here (see [4] for DNS using variable polynomial order elements). Typically, we use a stretched wall-normal mesh with

Table 1.
Run parameters for ℓVMS simulations.

Re_τ	L_x, L_y, L_z	$N_x \times N_y \times N_z$	p	c_s	Δy_w^+	Δx^+	Δz^+	d.o.f.
100	4π, 2, $4\pi/3$	$4 \times 4 \times 4$	5	7/4	2.2	314	105	13,824
100	4π, 2, $4\pi/3$	$4 \times 4 \times 4$	5	uniform	4.3	314	105	13,824
395	π, 2, $\pi/2$	$4 \times 6 \times 9$	5	7/4	2.3	310	103	46,656

$$y_j = \frac{\tanh(c_s(2j/N_y - 1))}{\tanh c_s} + 1, \qquad j = 0, 1, \ldots, N_y \tag{5}$$

where c_s is the stretching factor in the range $1.75 < c_s < 2.0$. Table 1 also lists the element spacings in the streamwise and spanwise directions (Δx^+ and Δz^+) as well as the distance of the first collocation point from the wall, Δy_w^+, all in wall-units. In all cases, we use third-order TVD-RK time advancement with $\Delta t = 0.0001$. This time step is a factor of 10 smaller than that typically used in our prior incompressible simulations [16] because the incompressible code treats wall-normal viscous terms implicitly. We are currently enhancing our DG code to support implicit time-advancement.

We use a constant coefficient Smagorinsky variant of the VMS model applied to the small-scales. The Smagorinsky coefficient is 0.1 and the length-scale in the eddy viscosity is computed using

$$\bar{\Delta}^2 = \frac{L_x L_z}{N_x N_z (p+1)^2} \tag{6}$$

which is designed to account both for element size as well as polynomial order. For all cases presented here, the 'large-scales' are represented by the first two-polynomial modes on each element (i.e. the constant and linear modes). This choice is made so that typical near-wall structures are well represented in the large-scale space [11]. The remaining modes on each element are taken as the 'small-scales' where the small-small variant of the Smagorinsky model is applied [6]. To help control aliasing errors in these high-order simulations, we use a Boyd-Vandeven spectral filter with a spectral shift of 4 (see [17]). We have also successfully employed over-integration [18] to de-alias our solutions and these results will be available in [12].

Mean and rms profiles for $Re_\tau = 100$ are shown in Fig. 1 using both a uniform and stretched mesh in the wall-normal direction. Even on the uniform mesh with the coarse near-wall resolution, $\Delta y_w^+ = 4.3$, the results are in reasonable agreement with DNS. The rms velocities clearly show the influence of the weak wall-boundary conditions in the streamwise direction with noticeable slip near the wall. As first presented in the context of DNS using DG [4], this is effectively a 'boundary layer capturing' method where the viscous sub-layer is captured by a discontinuity at the wall. This results in accurate mean and rms results without the need to resolve the viscous sublayer.

Figure 2 shows that mean and rms profiles for ℓVMS

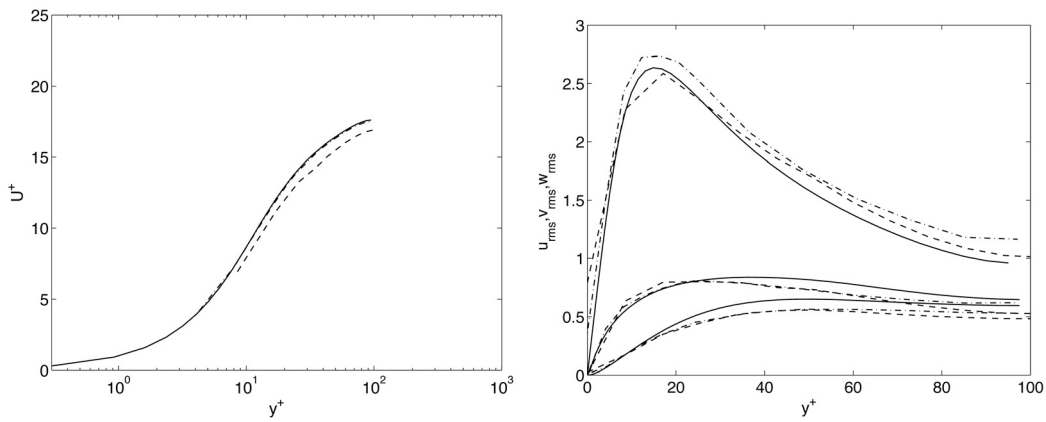

Fig. 1. Mean and rms velocity profiles for $Re_\tau = 100$ on $4 \times 4 \times 4$ mesh using $p = 5$: —— incompressible DNS; ---- ℓVMS with uniform wall-normal mesh; — - — ℓVMS with stretched wall-normal mesh.

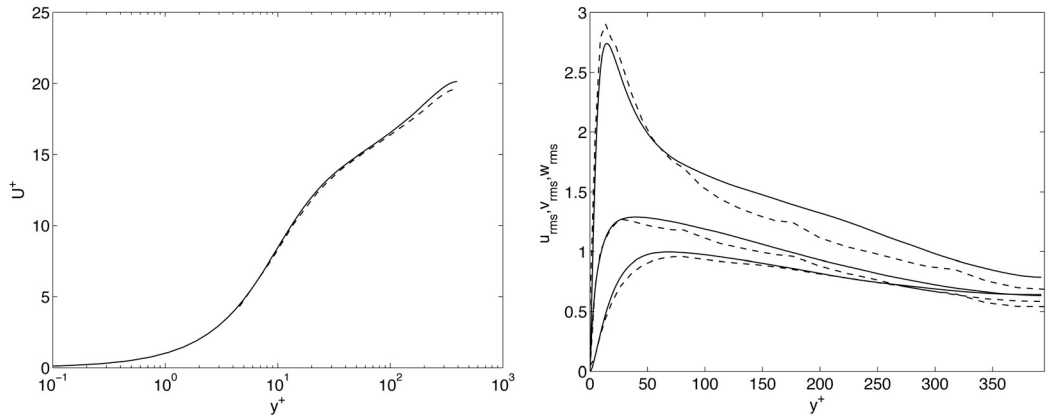

Fig. 2. Mean and rms velocity profiles for $Re_\tau = 395$ on $4 \times 6 \times 9$ mesh using $p = 5$: —— incompressible DNS [14]; ---- ℓVMS

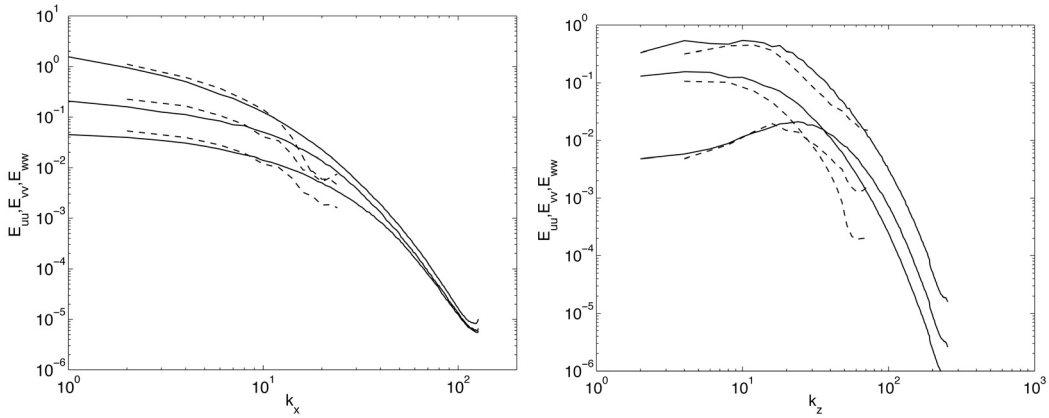

Fig. 3. Streamwise and spanwise velocity spectra for $Re_\tau = 395$ on $4 \times 6 \times 9$ mesh using $p = 5$: —— incompressible DNS [14]; ---- ℓVMS

at $Re_\tau = 395$ are also in good agreement with DNS. We emphasize that these results were obtained without tuning of any parameters. All that is required is to use the same relative resolution (see Table 1). We conclude by presenting streamwise and spanwise velocity spectra taken at $y^+ = 20$ (Fig. 3) for $Re_\tau = 395$ which show remarkably good agreement with DNS in the large-scales. Similar to prior VMS computations using global spectral-methods [11], energy in the small-scales is noticeably less than that of DNS. In VMS methods, the small-scales play the role of a buffer that protect the large-scales from modeling and truncation errors. This indeed appears to be the case in the current ℓVMS simulations, which, with an appropriately selected large-scale space and sufficiently large small-scale space (see [11]), result in excellent mean, rms, and large-scale spectra.

4. Conclusions

As a first-step toward ℓVMS simulations of turbulent flows, this paper presents ℓVMS results for planar channel flows that demonstrate excellent mean and second-order statistics. These results are obtained using a constant coefficient Smagorinsky model applied only to small-scales where the small-scales are defined local to each element. Similar to our experiences with global spectral methods and VMS, the main requirements are that the large-scale space be sufficient to represent the dynamically important scales, while the small-scale space is sufficiently large to provide an adequate buffer to protect the large-scales. The reader is referred to [11,12] for additional details. Specific to ℓVMS, we find that the weak imposition of wall-boundary conditions prevents the need to resolve the viscous sublayer both for DNS (as shown in [4]) and in ℓVMS. These initial results provide guidance for the use of ℓVMS for more

complex turbulent flows, and this is the direction of our future research.

Acknowledgments

This work was supported in part by the Stanford/NASA Center for Turbulence Research, by Texas ATP grant 003604–0011–2001, and by the Department of Energy. Computations were performed on an 82 processor Pentium IV Beowulf cluster that was purchased with the aid of NSF MRI grant 0116289–2001.

References

[1] Collis SS. The DG/VMS method for unified turbulence simulation. AIAA Paper 2002–3124, 2002.
[2] Collis SS. Discontinuous Galerkin methods for turbulence simulation. In: Proc of the 2002 Center for Turbulence Research Summer Program, 2002, pp. 155–167.
[3] Collis SS, Ghayour K. Discontinuous Galerkin for compressible DNS. ASME paper number FEDSM2003–45632, 2003.
[4] Ramakrishnan S, Collis SS. Multiscale modeling for turbulence simulation in complex geometries. AIAA Paper 2004–0241, January 2004.
[5] Collis SS. Monitoring unresolved scales in multiscale turbulence modeling. Phys Fluids 2001; 13(6):1800–1806.
[6] Hughes TJR, Mazzei L, Jansen KE. Large eddy simulation and the variational multiscale method. Comp Vis Sci 2000; 3:47–59.
[7] Hughes TJR, Oberai AA, Mazzei L. Large eddy simulation of turbulent channel flows by the variational multiscale method. Phys Fluids 2001; 13(6):1755–1754.
[8] Hirsch C. Numerical Computation of Internal and External Flows, Vol. I: Fundamentals of Numerical Discretization. New York: J Wiley & Sons, 1988.
[9] Bassi F, Rebay S. A high-order accurate discontinuous finite element method for the numerical solution of the compressible Navier–Stokes equations. J Comp Phys 1997; 131:267–279.
[10] Oberai AA, Hughes TJR. The variational multiscale formulation of LES: channel flow at $Re_\tau = 590$. AIAA 2002–1056, 2002.
[11] Ramakrishnan S, Collis SS. Partition selection in multiscale turbulence modeling. Phys Fluids, 2004 (submitted).
[12] Ramakrishnan S. Local Variational Multiscale Method for Turbulence Simulation. PhD thesis, Rice University, 2004.
[13] Kim J, Moin P, Moser R. Turbulence statistics in fully developed channel flow at low Reynolds number. J Fluid Mech 1987; 177:133–166.
[14] Moser RD, Kim J, Mansour NN. Direct numerical simulation of turbulent channel flow up to $Re_\tau = 590$. Phys Fluids 1999. 11:943.
[15] Coleman GN, Kim J, Moser RD. A numerical study of turbulent supersonic isothermal-wall channel flow. J Fluid Mech 1995; 305:159–83.
[16] Collis SS, Chang Y, Kellogg S, Prabhu RD. Large eddy simulation and turbulence control. AIAA Paper 2000–2564, 2000.
[17] Warburton T, Pavarino LF, Hesthaven JS. A pseudo-spectral scheme for the incompressible navier-stokes equations using unstructured nodal elements. J Comput Phys 2000; 164(1):1–21.
[18] Kirby RM, Karniadakis GE. De-aliasing on non-uniform grids: algorithms and applications. J Comp Phys 2003; 191:249–264.